FEATURES-BASED APPROACH FOR ALZHEIMER'S DISEASE DIAGNOSIS USING VISUAL PATTERN OF WATER DIFFUSION IN TENSOR DIFFUSION IMAGING

Olfa Ben Ahmed[⋆] *Jenny Benois-Pineau*[⋆] *Chokri Ben Amar*[†] *Michèle Allard* [⋆†] *Gwénaëlle Catheline* [⋆†]

[⋆] Laboratoire Bordelais de Recherche en Informatique, University of Bordeaux , France
[†] Research Groups on intelligent machines (ReGIM), University of Sfax, Tunisia
[⋆†] The Aquitaine Institute for Cognitive and Integrative Neuroscience, University of Bordeaux, France

ABSTRACT

In this paper, we propose a feature-based classification framework for Alzheimer's disease (AD) recognition using Tensor Diffusion Imaging (DTI). The main contribution consists in considering the visual pattern of water molecules diffusion in the most involved region in AD (hippocampal area). We use the Circular Harmonic Functions (CHFs) and the Bag-of-Visual-Words approach to build an AD related-signature. The experiments were accomplished first with a subset of participants from the Alzheimer's Disease Neuroimaging Initiative (ADNI) dataset and then with the DTI scans of a French epidemiological study: "Bordeaux-3City". Experimental results demonstrate that our features-based method applied on the MD maps is able to capture the AD-related atrophy and then classify between AD subjects.

Index Terms— Features, CHFs, SVMs, Alzheimer's disease, DTI, MD maps, hippocampus, AD-related signature

1. INTRODUCTION

Analysis of different Magnetic Resonance Imaging (MRI) modalities for AD research has been popular subject since the last decade [1, 2]. Brain structural changes in AD subjects at the group level has been well studied [3, 4], but the pattern classification of MRI scans across individuals still remains less developed. The main challenge here lies in the identification of features which provide the most reliable information about the particular disease (the so-called disease signature). Moreover, symptoms of the disease can vary between individuals, in this case individual scans patterns need to be taken into consideration and thus build a distinctive signature of disease-related atrophy per subject. Recently, a class of local features-based methods has demonstrated an impressive performance for Alzheimer's disease related signature extraction from structural MRI (sMRI) [5, 6, 7, 8, 9, 10, 11, 12]. Despite effectiveness of sMRI in detecting macro-structural loss for AD diagnosis, micro-structural changes remain invisible in structural scans. They can be delineated in other MRI modalities such as Tensor Diffusion Imaging (DTI). To the best of our knowledge, feature-based approach is not yet investigated on DTI for AD diagnosis. DTI is relatively a new Magnetic Resonance technique. It yields quantitative measures for tissue microstructure by measuring the diffusion information of water molecules in brain tissues [13]. Actually, the quantitative information about brain ultrastructure is given by quantifying isotropic and anisotropic water diffusion. Consequently, with this respect, DTI-derived maps such as the Mean Diffusivity (MD) image could be a diagnostic tool that quantifies the degree of tissue atrophy and thus could be a good biomarker for AD disease diagnosis.

Hippocampus is one of the first brain regions to be affected by AD pathology, and microstructural alterations within hippocampus have been quantified in vivo using DTI. MD, as a marker of microstructure, appears to be a more sensitive marker of hippocampal integrity than macrostructural measurements with MR volumetry [14]. Referring to the domain knowledge; when a brain is affected by Alzheimer's disease, the hippocampus undergoes a cells degeneration and then water molecules become less hindered because of loss of structural barriers to water molecular motion. In this case we hypothesize that the fast diffusion of water on the hippocampal area is illustrated by an hyper-signal (brighter pixels) on the MD maps. Hence, from MD maps, it is possible to extract features and build visual signature to distinguish between an affected and a healthy hippocampus. In this paper, we propose a machine learning framework to build meaningful medical signature associated with visual appearance of MD maps for Alzheimer's disease diagnosis research.

2. FEATURE-BASED CLASSIFICATION APPROACH

Our goal is to build a visual signature related to the hippocampus atrophy from the MD map. Hence, the MD images has to be processed to allow for ROI selection using a normalized anatomical atlas.

2.1. Preprocessing

For each subject, preprocessing of DTI included corrections for eddy currents and head motion, skull stripping with the Brain Extraction Tool (BET) and fitting of diffusion tensors

to the data with DTIfit module of the Software Library FSL [1]. Fitting step allows the generation of the MD and FA maps. In the current research, we retain only the MD maps. All MD image preprocessing steps were performed using Statistical Parametric Mapping (SPM8, Welcome Department of Imaging Neuroscience, London, UK;)[2] running on MATLAB (MathWorks, Sherborn,MA, USA). After MD images alignment whose purpose is to adjust movement between slices of DTI-derived maps. MD images were affinely coregistered to the corresponding anatomical scans using the default parameters of SPM. Indeed, anatomical scans were normalized onto the T1 template in MNI (Montreal Neurological Institute) brain template using the VBM8 toolbox [3] implemented in SPM8, and the resulting transformation parameters were applied to the subjects corresponding coregistered MD maps. Finally, the spatially normalized MD maps were smoothed with a Gaussian filter to improve Signal-to-Noise-Ratio (SNR) using the smoothing module of SPM.

2.2. Features extraction and signature generation

As we experimented in [10], conventional SIFT and SURF descriptors are less adapted for atrophy description in MRI. Here, we resort to the use of Circular Harmonic Functions (CHFs) [15] decomposition of MD maps signal. CHFs were used for selection of contrasted patterns in brains. Laguerre Gauss-CHFs is a set of orthogonal complex functions defined on the real plane. Thus, the MRI slice $S(x_0, y_0)$ can be expanded in the analysis point x_0 , y_0 for a fixed scale σ in Cartesian system as follows:

$$S(x_0, y_0) = \sum_{\alpha=-\infty}^{\infty} \sum_{n=0}^{\infty} g_{\alpha,n}(x_0, y_0; \sigma) \Psi_n^{\alpha}(r, \theta, \sigma), \quad (1)$$

where

$$g_{\alpha,n}(x_0, y_0; \sigma) = \int_{-\infty}^{\infty} \int_{-\infty}^{\infty} S(x_0, y_0) \overline{\Psi_n^{\alpha}(r, \theta, \sigma)} dx dy,$$

And

$$r = \sqrt{(x - x_0)^2 + (y - y_0)^2},$$

$$\theta = arctg(\frac{y - y_0}{x - x_0})$$

The coefficients $g_{\alpha,n}$ of the partial expansion of local neighborhood can be used as a feature descriptor. The advantages of these features are such that they capture both the direction and smooth variations of image signal.

The hippocampus ROI was selected using an atlas of label normalized in MNI. Then, hippocampus features were computed on MD map by the development of the MD image signal on the basis of Circular Harmonic Functions (CHFs). We use a "dense sampling" strategy to capture all the relevant information. We perform 2D CHFs transform computation slice-by-slice. Hence the whole description of the hippocampal is a collection of 2D CHFs descriptors for each slice and each projection.

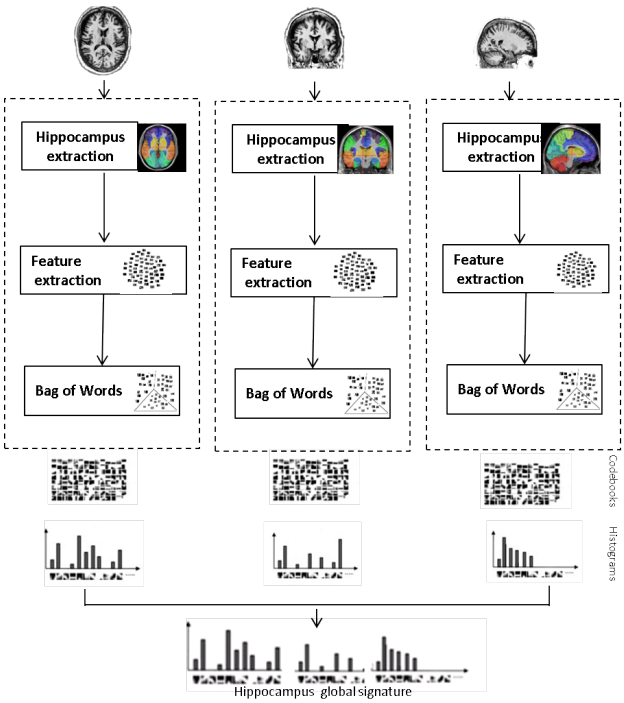

Fig. 1. AD-related signature generation, hippocampus description from the MD maps

Figure 1 illustrates the visual signature generation. Here, we use the Bag-of-Visual-Words (BoVW) method [16] to build signature upon CHFs descriptors. Figure 2 shows the CHFs features placement on the hippocampus ROI from a a slice in a sagittal projection of an MD map. The extracted feature points "support areas" (i.e. where the descriptors are computed) are denoted with blue circles. To integrate atrophy information from different projections (sagittal, axial and coronal), we propose to construct a separate codebook for MRI scans within each projection. Then, a ROI is described by a concatenation of the obtained BoVW histograms. The dimension of the obtained signature is reduced using the

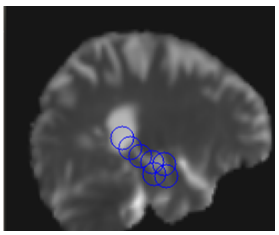

Fig. 2. CHFs features detection in a sagittal slice of an MD map

[1] http://www.fmrib.ox.ac.uk/fsl
[2] http://www.fil.ion.ucl.ac.uk/spm
[3] http://dbm.neuro.uni-jena.de/vbm8/)

Table 1. Demographic description of the ADNI group. Values are denoted as mean ± standard deviation

Diagnosis	Number	Age	Gender (M/F)	MMSE
AD	24	68 ±5.3	10/14	24.1±2.4
NC	25	72.3±3	12/13	29.7±1.3
MCI	21	73 ±2.9	8/13	27±0.8

conventional PCA technique [17]. Support Vector Machines [18] are used to classify subjects, we are interested in the binary classification (AD versus Normal Control (NC)), (NC versus Mild Cognitive Impairment (MCI)) and (AD versus MCI). The MCI group is an heterogeneous class presenting a transitional stage between NC and AD.

3. IMAGING DATA

Data used in the experiments of the current research come from two sources. First, we used a subset of the Alzheimer's Disease Neuroimaging Initiative (ADNI) dataset. Is is to note that the ADNI recently added diffusion tensor imaging (DTI), among several other new imaging modalities, in an effort to identify sensitive biomarkers of Alzheimer's disease (AD). Second, we used a 10-year follow-up of a population-based cohort (Bordeaux-3City) from the Three-City (3C) study [19]. Moreover, only baseline images have been used in the current work. Also, only one scan per subject has been used. We selected from the ADNI data 25 NC, 24 AD and 21 MCI DTI and their corresponding structural MRI. Where for the "Bordeaux-3City", we selected 21 NC subjects. However, for the AD group, we have only 7 DTI scans with their corresponding structural MRI. Table 1 and Table 2 present a summary of the demographic characteristics of the studied groups (including the number, age, gender and MMSE of the subjects). The Mini Mental State Examination (MMSE) is a psychological test quantifying the cognitive function. The number of scans available for this work was limited by the availability of DTI data. In fact, the DTI is a relatively new MR modality, and not all subjects has both DTI and sMRI scans.

Table 2. Demographic description of "Bordeaux-3City" group. Values are denoted as mean ± standard deviation

Diagnosis	Number	Age	Gender (M/F)	MMSE
AD	7	85.5 ±3	2/5	25.57 ±2.4
NC	21	82.7 ±4.5	9/12	27±1

4. EXPERIMENTS AND RESULTS

4.1. Dimensionality reduction

To reduce signatures dimensionality, we consider percentages of total energy which is obtained from cumulative energy vector. As the percentage of energy is reduced, the number of coefficients required also dramatically reduces, and according the candidate feature vector size is reduced for classification. For instance, the ADNI group signature's size is equal to 600 = 200 x 3 with 200 is the codebook size. Whereas the size of signature for the "Bordeaux-3City" data is 450 = 150 x 3 with 150 is the codebook size. Therefore, using PCA the signatures sizes were reduced by keeping 95% of energy. Hence, we obtained a signatures sizes equal to 34 and to 22 respectively for the ADNI and the "Bordeaux-3City" groups.

4.2. Codebook size Variation

In a second part of experiments, we plot the variation of classification accuracy (AD vs NC, NC vs MCI and MCI vs AD) function to the codebook size changes (Figure 3). In most cases, the accuracy can be improved with a larger codebook size, but it can also decrease in certain cases. In general, the accuracy does not change significantly with codebook size. A similar trend has been observed for The **"Bordeaux-3City"** data. Hence, we set the codebook sizes to 200 and 150 respectively for ADNI and "Bordeaux-3City" groups.

4.3. SVM classification

Parameter setting for SVM is critical to obtain good performance. Hence, training SVM we need to select optimal kernel function parameters as well as soft margin parameter C. We choose to use a grid search on the log ratio of the parameters associated with cross validation. Then, value pairs (C, γ) are assessed using cross validation and then the pair with highest accuracy is chosen. In this paper, we used 10 folds cross validations to evaluate classification performance. We repeated the 10 fold cross-validation 10 times for a more general performance estimation of the classifier. Each time the 10 randomly selected folds were generated and the final result was the average accuracy, sensitivity and specificity of the 10 experiments. Table 3 and Table 4 present the classification results in terms of sensitivity, specificity, accuracy and BAC metrics with 95% confidence interval for respectively the ADNI and "Bordeaux-3City" groups.

4.3.1. Classification results for (NC vs. AD)

In this section, we present the classification results obtained in the first experiment, which consisted in distinguishing between NC and AD subjects. Our method achieved classification accuracies of 86.73% and 80.34% respectively for the ADNI subset and "Bordeaux-3City" data. We reported for the subset a specificity 98% of and a sensitivity of 75%. Indeed, for "Bordeaux-3City" data, we reported a hight specificity (90.91%) but lower sensitivity. This could be caused by the small number of AD subjects compared to the number of Normal Control used in this experiment.

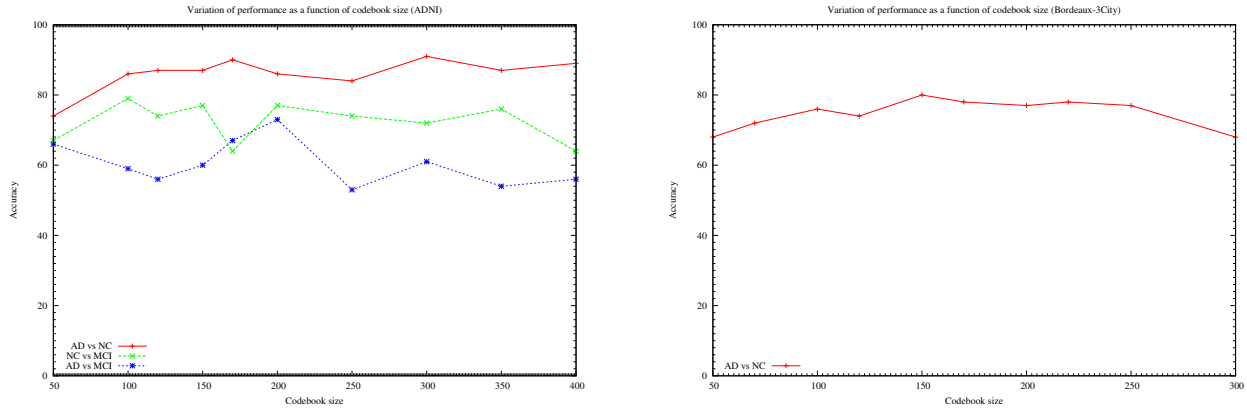

Fig. 3. Codebook variation for the ADNI dataset and Bordeaux-3City group

Table 3. Classification results: AD versus NC, MCI versus NC and AD versus MCI (ADNI)

	AD versus NC	**NC versus MCI**	**AD versus MCI**
Accuracy %[95% CI]	86.73 [86.10 87.37]	77.39[75.67 79.12]	73.11[71.32 74.90]
Specificity %[95% CI]	98 [96.76 99.24]	89.20 [86.97 91.43]	77.92[76.26 79.57]
Sensitivity %[95% CI]	75[74 75]	63.33 [60.68 65.99]	67.62[63.7 71. 53]
BAC (%)	86.5	76.27	72.77

4.3.2. Classification results for (NC vs. MCI)

A high specificity is obtained for the NC versus MCI classification (89.20%). In addition, an accuracy of 77.39% and a sensitivity of 63.33% were reported.

Table 4. Classification results: AD versus NC (Bordeaux-3City)

Accuracy %[95%CI]	80.34 [77.47 83.22]
Specificity %[95%CI]	90.91 [88.09 93.73]
Sensitivity %[95%CI]	47.14 [43.09 51.20]
BAC (%)	69.03

4.3.3. Classification results for (AD vs. MCI)

The most difficult classification task concerning the ADNI subset is to distinguish AD from MCI patients. We obtained an accuracy of 73.11%, a specificity of 77.92% and a sensitivity of 67.62%. This is presumably due to the fact that MCI is a transitory heterogeneous stage between NC and AD.

Despite the DTI modality is of much lower visual quality (blurred and luck of details) and associated with low SNR compared to structural MRI (the SNR values calculated on the ADNI group were 37 and 32 respectively for the preprocessed sMRI and the MD maps), we have shown that CHFs features allow for application of features-based method and provide a robust representation of AD-related atrophy from the MD maps. Note that typical performance figures of features-based method on structural MRI from the same ADNI group give accuracies of 73% and 68.26%, and BACs of 78.2% and 75% respectively for NC versus MCI and AD versus AD classification problems. In addition, the BoVW approach proved to be effective in explaining the visual richness of MD images and relations between visual patterns and their semantic meaning. Alone, the MD maps show rather high classification scores. Furthermore, our approach, do not require a precise segmentation of ROI, performs well not only on sMRI, what we showed in our previous work [10], but also on more challenging modality such as MD maps. Combining DTI data with structural findings should further increase its diagnosis performance. However, without the aid of the sMRI, the anatomical information of the hippocampus acquired by MD maps is difficult to interpret due to the lack of anatomical information in this modality.

5. CONCLUSION

In this paper, we introduced an approach of an AD-related signature generation of hippocampus ROI on MD maps of DTI modality. This information was used to effectively discriminate the MCI and AD patients from NC, as well as between the MCI and AD patients. The present research is the first attempt (in our best knowledge) to apply features-based approaches on this modality for AD diagnosis. We used the CHFs to extract content from the DTI map: MD. The obtained

results are encouraging and open interesting perspectives. In the perspective of this work we will proceed with fusion of different modalities in a global classification framework.

6. REFERENCES

[1] Zhengjia Dai, Chaogan Yan, Zhiqun Wang, Jinhui Wang, Mingrui Xia, Kuncheng Li, and Yong He, "Discriminative analysis of early alzheimer's disease using multi-modal imaging and multi-level characterization with multi-classifier (m3)," *Neuroimage*, vol. 59, no. 3, pp. 2187–2195, 2012.

[2] D. Zhang, Y. Wang, L. Zhou, H. Yuan, and D. Shen, "Multimodal classification of alzheimer's disease and mild cognitive impairment," *NeuroImage*, vol. 55, no. 3, pp. 856–867, 2011.

[3] John Ashburner and Karl J. Friston, "Voxel-Based Morphometrythe methods," *Neuroimage*, vol. 11, pp. 805–821, 2000.

[4] Rémi Cuingnet, Emilie Gerardin, J érme Tessieras, and et al, "Automatic classification of patients with Alzheimer's disease from structural MRI: A comparison of ten methods using the ADNI database.," *NeuroImage*, vol. 56, no. 2, pp. 766–781, 2011.

[5] Mayank Agarwal and Javed Mostafa, "Image retrieval for Alzheimer disease detection," in *Proceedings of the First MICCAI international conference on Medical Content-Based Retrieval for Clinical Decision Support*, Berlin, Heidelberg, 2010, MCBR-CDS'09, pp. 49–60, Springer-Verlag.

[6] Mohammad Reza Daliri, "Automated Diagnosis of Alzheimer disease using the Scale-Invariant Feature Transforms in Magnetic Resonance Images," *J. Med. Syst.*, vol. 36, no. 2, pp. 995–1000, 2012.

[7] Olfa Ben Ahmed, Jenny Benois-Pineau, Chokri Ben Amar, Michelle Allard, and Gwénaëlle Catheline, "Early Alzheimer disease detection with bag-of-visual-words and hybrid fusion on structural MRI," in *CBMI'2013*, 2013, pp. 79–83.

[8] Andrea Rueda, John E. Arevalo, Angel Cruz-Roa, Eduardo Romero, and Fabio A. González, "Bag of features for automatic classification of Alzheimer's disease in Magnetic Resonance Images," in *CIARP*, 2012, pp. 559–566.

[9] Devrim Unay, Ahmet Ekin, and Radu S. Jasinschi, "Local structure-based region-of-interest retrieval in brain MR images," *IEEE Transactions on Information Technology in Biomedicine*, vol. 14, no. 4, pp. 897–903, 2010.

[10] Olfa Ben Ahmed, Jenny Benois-Pineau, Michle Allard, Chokri Ben Amar, and Gwénaëlle Catheline, "Classification of alzheimers disease subjects from mri using hippocampal visual features," *Multimedia Tools and Applications*, pp. 1–18, 2014.

[11] Ye Chen, Judd Storrs, Lirong Tan, Lawrence J. Mazlack, Jing-Huei Lee, and Long J. Lu, "Detecting brain structural changes as biomarker from magnetic resonance images using a local feature based svm approach," *Journal of Neuroscience Methods*, vol. 221, no. 0, pp. 22 – 31, 2014.

[12] Olfa Ben Ahmed, Jenny Benois-Pineau, Chokri Ben Amar, Michelle Allard, and Gwénaëlle Catheline, "Alzheimer disease detection on structural MRI," in *In the Proceedings of ESMRMB 2013 Congress, Toulouse, France*, 2013, p. 87.

[13] Denis Le Bihan, "Looking into the functional architecture of the brain with diffusion MRI," *Nature Reviews. Neuroscience*, vol. 4, pp. 469–80, jun 2003.

[14] Lies Clerx, Pieter Jelle Visser, Frans Verhey, and Pauline Aalten, "New mri markers for alzheimer's disease: A meta-analysis of diffusion tensor imaging and a comparison with medial temporal lobe measurements," *Journal of Alzheimer's Disease*, vol. 29, no. 2, pp. 405429, 2011.

[15] Dmitry V. Sorokin, Maxim . Mizotin, and Andrey S. Krylov, "Gauss-laguerre keypoints extraction using fast hermite projection method," in *Proceedings of the 8th international conference on Image analysis and recognition - Volume Part I*, Berlin, Heidelberg, 2011, ICIAR'11, pp. 284–293, Springer-Verlag.

[16] Gabriella Csurka, Christopher R. Dance, Lixin Fan, and et al, "Visual categorization with bags of keypoints," in *Workshop on Statistical Learning in Computer Vision, ECCV*, 2004, pp. 1–22.

[17] I. T. Jolliffe, *Principal Component Analysis*, Springer, second edition, Oct. 2002.

[18] Bernhard Scholkopf and Alexander J. Smola, *Learning with Kernels: Support Vector Machines, Regularization, Optimization, and Beyond*, MIT Press, Cambridge, MA, USA, 2001.

[19] Amandine Pelletier, Olivier Periot, Bixente Dilharreguy, Bassem Hiba, Martine Bordessoules, Karine Pérès, Helene Amieva, Jean-Franois Dartigues, Michele Allard, and Gwénaëlle Catheline, "Structural hippocampal network alterations during healthy aging: A multi-modal mri study," *Frontiers in Aging Neuroscience*, vol. 5, pp. 84, 2013.